JOURNAL OF MECHANICS OF CONTINUA AND MATHEMATICAL SCIENCES
www.journalimcms.org

ISSN (Online) : 2454 -7190 Vol.-20, No.-8, August (2025) pp 152 - 165 ISSN (Print) 0973-8975

DESIGN AND DEVELOPMENT OF THE PIEZOACOUSTIC RESPONSE OF ALUMINIUM NITRIDE FOR ENHANCED ULTRASOUND DEVICES

J. Manga[1], V.J.K. Kishor Sonti [2]

[1,2] Department of ECE, Sathyabama Institute of Science and Technology,Chennai, India.

Email : [1]jangidimanga@gmail.com, [2]kishoresonti.ece@sathyabama.ac.in

Corresponding Author: **J. Manga**

https://doi.org/10.26782/jmcms.2025.08.00011

(Received: June 01, 2025; Revised: July 27, 2025; Accepted: August 09, 2025)

Abstract

Piezoelectric materials are integral to ultrasound probes and scanning devices in medical imaging and fingerprint recognition, as they can convert mechanical energy into electrical energy. This conversion enables the imaging of internal structures, facilitating medical diagnostics by highlighting deviations from normal organ dimensions. Traditionally, Lead Zirconate Titanate (PZT-4) has been used in handheld ultrasound probes, despite its low output and significant environmental hazards upon disposal. This paper presents Aluminium Nitride (AlN) as a safer, environmentally friendly, and thermally stable alternative. AlN is compatible with Complementary Metal Oxide Semiconductor (CMOS) technology, making it a viable option for sophisticated ultrasound probes that can be compact enough to be taken into the body. The simulations conducted through COMSOL Multiphysics at 200 kHz, this study demonstrate AlN's piezo acoustic properties, which are crucial for generating photoacoustic images in biomedical imaging. The presented simulation model enables monitoring of the material's acoustic behavior in response to specific electrical inputs and frequencies.

Keywords: Piezoelectric, Ultrasound, Aluminium nitride, COMSOL Multiphysics, Frequency, Acoustic

I. Introduction

The ultrasound machines account for cost-effective sensing in the fields of industry, agriculture, and 2D and 3D ranging [A. Abu-libdeh, and A. Emadi, et al. (2022)], biomedical imaging [W. Lee, and Y .Roh et al. (2017)], fingerprint detection [A. Iula, (2019)], and non-destructive testing[M. Lethiecq et al., (2008); M. Darmon, et al. (2022)]. The ultrasound devices consist of piezoelectric transducers [D. O. Urroz-Montoya, et al. (2019)], which works on the principle of the piezoelectric effect[D. O. Urroz-Montoya, et al. (2019)] that is, when stress is applied to the material, an electric potential is generated and vice-versa. These piezoelectric transducers are fabricated inside the ultrasound probes as microelements that consist of a CMOS-based [E. Ledesma, et al. (2021)] process. An array of such

microtransducers is used in tracking the response accurately. The piezoelectric materials used in such a setup are mainly lead zirconate titanite (PZT) [C. Cheng, et al. (2021)] and aluminum nitride (AlN) [Xin Su et al. 22].

However, considering the less hazardous nature of AlN can be effectively used in medical probes. The usage of PZT has been an old method. The main toxic impact of PZT is marine sediment eco-toxicity [A. Safari, Q. Zhou, et al. (2023)], and most of the environmental impact comes from primary energy consumption while manufacturing PZT. PZT-based piezoelectric micromachined ultrasonic transducers (pMUTs) offer advantages like high piezoelectric coefficients ($d_{31} \approx 40–110$ pm/V) for enhanced sensitivity but face several critical limitations [Q. Yu *et al.*, (2022)]. PZT requires high-temperature processing (>650°C), making integration with CMOS electronics difficult without specialized steps. Ceramic PZT's brittleness raises reliability issues in endoscopic or portable medical devices.[H. Wang, Z. Chen, et al. (2020)] Sputtered PZT films suffer from high intrinsic stress and low deposition rates compared to AlN. [J. Pan, C. Bai, et al. (2023)]. These limitations drive ongoing research into new designs with alternative materials like AlN for CMOS-compatible applications.[F. Pop, B. Herrera, et al. (2020)]

In this research work, an Aluminium Nitride piezo-electric material-a single-element transducer design- is demonstrated with its modelling in COMSOL. This model recreates a quarter-half plate in such a design. The component is rotationally symmetric, making it conceivable to set up the model as a 2D pivotally symmetric issue. The proposed research contributes to the development and application of AlN-based micromachined ultrasonic transducers by improving their acoustic field performance. The optimized structure[C. Fei et al. (2016)] and electrode distribution can lead to more uniform and symmetrical radiation beams, enhancing the transducer's functionality in various applications. This leads to the discussion of different piezo-acoustic transducers.

II. Piezoacoustic Transducers

Piezoelectric transducers, sometimes referred to as piezoacoustic transducers, are devices that use the piezoelectric effect to transform electrical energy into mechanical energy (sound waves) and vice versa. These transducers find widespread use in a variety of domains, such as medical imaging, non-destructive testing, industrial automation, and sonar systems. In contrast, the material produces an electric charge when mechanical tension is applied. This bidirectional property allows piezoacoustic transducers to function as both transmitters and receivers of acoustic signals.

There are two typesofPiezoacousticTransducers

II.i. Single-Component Transducers:

Single-component transducers [E. G. Nesvijski (2000)] consists of a single piezoelectric element. This design is particularly advantageous for applications where a focused or narrow beam width is essential [B. Herrera, P. Simeoni, et al. (2022)]. For instance, in medical imaging, these transducers can provide detailed images of specific areas within the body, aiding in precise diagnosis and treatment. Similarly, in

sonar applications, single-component transducers are used to focus sound waves in a tight beam, enabling the detection and identification of objects or features in underwater environments. Their simplicity and effectiveness make them ideal for tasks that require concentrated energy and pinpoint accuracy.

II.ii. ArrayTransducers:

Array transducers[J. Y. Pyun, Y. H. Kim et al. (2023)], on the other hand, are composed of multiple piezoelectric elements arranged in as pecific pattern or cluster. This configuration allows for greater flexibility and capability in various applications. In medical ultrasound, array transducers enable high-resolution imaging and wide-area coverage, which are crucial for detailed examinations and comprehensive diagnostics. These transducers can be dynamically operated, adjusting the focus and direction of the sound waves to capture detailed images of different tissues and organs. In under watersonar[M. Ishikawa et al. (2005)], array transducers provide extensive area coverage, making them suitable for mapping large regions and detecting objects over a broad expanse. The ability to control and manipulate the beam pattern enhances their performance in both medical and sonar applications, offering superior imaging and detection capabilities.

II.iii. Materials for Transducers:

AlN and PZT transducers exhibit distinct resonant and bandwidth characteristics when analyzed in COMSOL, particularly around 200 kHz. AlN, with its high stiffness (Young's modulus ~345 GPa) and low damping, demonstrates a sharp resonant peak and narrow bandwidth (Q-factor >1000), making it ideal for high-frequency sensors and filters. COMSOL simulations reveal a steep impedance dip at resonance, as shown in studies like Piazza et al. (2019), where AlN resonators achieved precise frequency control but limited operational bandwidth (<1% of center frequency). In contrast, **PZT** leverages its high piezoelectric coefficients (d_{33} ~200–600 pC/N) and softer structure (Young's modulus ~60–80 GPa) to deliver **broader bandwidths** (5–10% at 200 kHz) with a flatter impedance response. This makes PZT better suited for applications such as ultrasound imaging, where a wider bandwidth improves resolution.

The trade-offs between materials are evident in COMSOL frequency sweeps: AlN's **high-Q resonance** ensures efficiency in narrowband systems, while PZT's **damping and electromechanical coupling** favor broadband energy transduction. For instance, Sherrit et al. (2012) highlighted PZT's superior performance in actuators due to its ability to sustain wider frequency ranges. When designing transducers at 200 kHz, AlN's thin-film requirement (~10 µm) contrasts with PZT's thicker layers (~50–100 µm), influencing device scalability and integration. References like Tadigadapa et al. (2009) further emphasize AlN's advantage in MEMS resonators, while PZT dominates in high-output, loss-tolerant applications.

AlN is a lead-free alternative, making it attractive for biomedical implants and wearable devices (Piazza et al., 2019). However, its low coupling coefficient (k_t ~ 0.2–0.3) reduces energy efficiency, and its narrow bandwidth (5–15%) limits imaging resolution (Muralt, 2008). AlN's acoustic impedance (~34 MRayl) is closer to tissue

than PZT, but it still requires impedance matching for optimal performance. A key advantage is its CMOS-compatibility, enabling MEMS-based ultrasound arrays (Lu et al., 2021). However, thin-film AlN struggles with high-power applications due to breakdown risks.

II.iv. Target study

The goal of this study is to provide a comprehensive comparison between aluminum nitride (AlN) and lead zirconate titanate (PZT) piezoelectric materials for 200 kHz diagnostic ultrasound applications, evaluating their suitability based on key performance metrics and application requirements. Specifically, we assess AlN's advantages in CMOS-compatible fabrication and biocompatibility (Piazza et al., 2019) against PZT's superior electromechanical coupling and power handling capabilities (Smith & Auld, 1991). The analysis focuses on four critical aspects: (1) acoustic performance (Shung, 2015), (2) environmental and biocompatibility considerations, (3) integration potential for miniaturized systems (Muralt, 2008), and (4) practical fabrication challenges and scalability. By systematically comparing these factors, this work aims to establish clear guidelines for material selection in 200 kHz ultrasound applications, whether for medical imaging requiring high sensitivity (favoring PZT) or for emerging wearable technologies demanding miniaturization and biocompatibility (favoring AlN). The findings will help researchers and engineers optimize transducer design based on specific application needs, from therapeutic ultrasound to implantable sensors. In terms of thermal stability, AlN outperforms PZT due to its high melting point (~2200°C) and lower thermal coefficient of delay (TCD), making it suitable for harsh environments. PZT, on the other hand, can suffer from performance degradation at elevated temperatures. Additionally, AlN is biocompatible and CMOS-compatible, allowing for integration into semiconductor processes and medical implants, whereas PZT contains toxic lead, restricting its use in eco-friendly and biomedical applications.

III. Model Structure

III.i Design flow through COMSOL

The process shown in Figure 1 illustrates the detailed COMSOL model starting from creating a model from the starting wizard, geometry of Piezo material, i.e, Aluminium Nitride, Acoustic layer, Perfect Matched layer. The physics definition of solid mechanics, electrostatics, and acoustics, boundary conditions for a perfectly matched layer and air medium, followed by meshing involved, and the required study in the time domain and acoustic domain, and finally, compute the results.

A piezoelectric transducer can be utilized either to change an electric flow to an acoustic tension field[E. G. Nesvijski, et al. (2000)], or the inverse, to create an electric flow from an acoustic field. These gadgets are, by and large, helpful for applications that require the measurement of sound in air and fluids. In a staged cluster ultrasound gadget, the piezo-electric plate gets into the plan through a progression of piled layers that are separated into columns. The interjection between these layers is represented as the kerf, and the columns are rehashed with a periodicity or pitch.[A. Guedes, et al. (2011)]

Figure 2 demonstrates the actual model designed for the experiment carried out in this paper. First, a Piezoelectric material of Aluminium Nitride was selected [J. Kim et al. (2022)]with valid conditions, then the model for acoustics is built on it with a medium of air and a perfectly matched layer to observe its behavior.

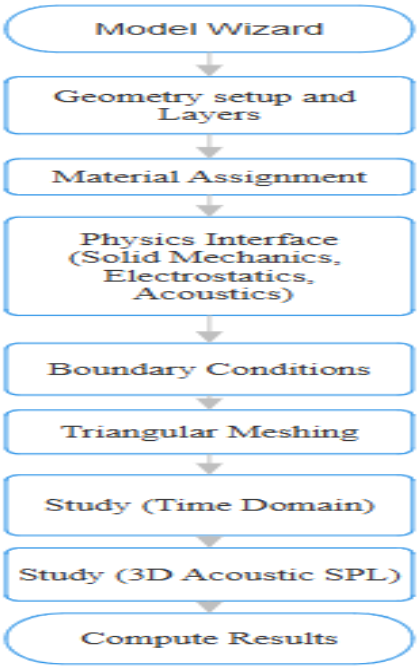

Fig.1. Flow diagram

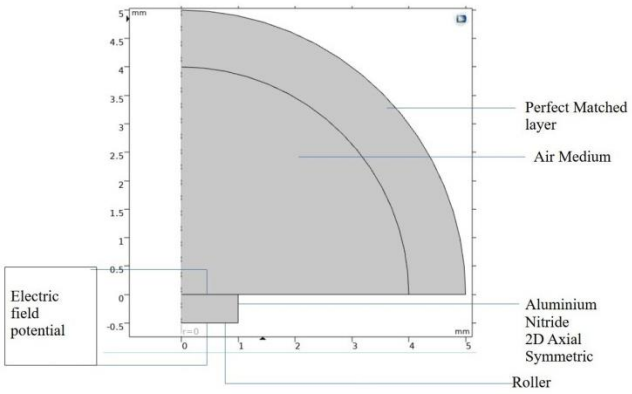

Fig. 2. The Model Outline

III.ii. Physics behind the model

Three basic material science interfaces—Pressure Acoustics, Solid Mechanics, and Electrostatics—are included in the model, which introduces the hidden acoustic-piezoelectric connection [H. Wang (2021)] [Akasheh, et al. (2024)], a recurrence area multiphysics interface. Primary acoustic pressure defines the wave condition in

the fluid domain surrounding the transducer. The latter two demonstrate the piezoelectric action.

The acoustic pressure approximation is depicted by the following wave equation:

$$\nabla \cdot \left(\frac{-1}{\rho_0}(\nabla p)\right) - \frac{\omega^2 p}{\rho_0 {c_s}^2} = 0 \quad (1)$$

Where ∇ is the operator, ρ_0 is the density in the air, p is the pressure, and c_s is the velocity of sound

This condition is settled by the Pressure Acoustics, Frequency Domainre presentation.

The piezoelectric structure consists of the material, Aluminium Nitride, which is an improved material for piezo electric devices. The piezo electric material is shown by handling the Solid Mechanics and Electrostatics interfaces [Y. Li, T. Omori, et al. (2022)]that are coupled through straight constitutive circumstances that partner stresses and strains to electric dislodging and electric field. These two domains address the equilibrium of body powers and volume charge density individually, as presented in the Equations as

$$\nabla \cdot \sigma = 0 \quad (2)$$

$$\nabla \cdot D = 0 \quad (3)$$

In COMSOL Multiphysics, this coupling is naturally executed by the Piezoelectric Impact point situated under the Multiphysics space [Aldrich, J.E. et al. (2007)]. The primary and electrical examinations are also time-consonant. In structural mechanics, it is recognized as frequency response analysis, whereas in electrical design, it is referred to as frequency domain analysis.[Q. Zhou et al. (2014).In this model, the excitation recurrence is assigned to be 200 kHz, which is in the ultra sonicrange.

III.iii. Limitingfactorsofthemodel

The transducer's base portion is grounded, and its top surface receives a 100-volt alternating current. To push the air domain, the solid parametric boundary's structural acceleration is employed.

At the connection point between the air and the piezoarea, the ordinary part of the underlying speed increase at the limit of the base material is used to drive the airspace [J. Cai et al. (2023)] [F. Pop, B. Herrera, et al. (2022)]. This relationship is communicated by the accompanying condition:

$$n \cdot \left(\frac{1}{\rho_0}(\nabla p)\right) = a_n \quad (4)$$

a_n is the increased speed factor in Equation 4

The acoustic strain[F. Pop, B. Herrera, et al. (2022)] at the point of interaction between the air and piezo material space acts as a limit load on the piezomaterial,

$$n \cdot \sigma = p \quad (5)$$

The bidirectional coupling at the piezo and air interface limits is naturally dealt with by the Acoustic-Construction limit hub situated under the Multi physics branch when you utilize the implicit Acoustic-Piezo electric relations, Frequency domain inter face [J. Jung, W. Lee, et al. (2017)]. The point of interaction limits is naturally recognized once you give suitable partitions of the model to the Pressure Acoustics, Frequency Domain, and Solid Mechanics interfaces, respectively [R. Manwar, et al. (2020)] [Neprokin, A. et al. (2022)]. The mathematics involved in the geometry of the model illustrates the computed acoustics in two-dimensional and three-dimensional acoustic pressure.

IV. Results and Discussion

COMSOL Multiphysics allows for the modelling of various physical phenomena, including piezoelectric materials. One of the special characteristics of piezoelectric materials is that the produce an electric charge when they are mechanically stressed and deform mechanically when they come into contact with an electric field. In COMSOL, one can model these coupled acoustic and structural perturbations in piezoelectric materials.

In this work, a simulation of a piezoacoustic field is studied that is caused by structural waves generated in a piezoelectric material. This gives an understanding of the behavior of piezoelectric materials in different environments, such as in water or air. The software provides a user-friendly interface for creating geometries, setting up material properties, and defining boundary conditions, making it suitable for both beginners and experience dengineers.

IV.i. Stressin Piezoelectric Material

The simulation of a simple piezoelectric crystal using COMSOL for understanding its mechanical stress and electric behavior is observed by fixing one end of the material. To give a general analysis of a piezoelectric crystal, an element is modelled in Figure 2, which is a 2-dimensional solid structure, with AlN material, and an applied electric voltage. The model featured a width of 10 mm and a height of 0.5mm. The thickness of the material is 0.005m. After the solid structure selection of the device is done, it is required to apply proper boundary conditions. The top layer is taken as floating potential, and the bottom is considered to be grounded electrically. In the electrostatics window, of plane thickness is chosen as 0.005m. The multiphysics section showed a solid mechanics and electrostatics prevalence. The meshing done on this material is to capture the stress variations observed on the application of an electrical potential.

At time 0s, that is initially, there is no stress shown on the material, and so it appears in a colour map as light green. In the next instances shown in Figure 2, the deformation is observed going from top to bottom on the extreme right side of the bar of a piezoelectric element.

The electrical potential observed on a plot in an export window is a sinusoidal variation as given in Figure 3. The observed values are entered into a text document showing the instantaneous values. Figure 3 and Figure4indicate the electric potential variation applied to the piezoelectric material that is used for generating stress on the

piezoelectric meshed bar on the edge, which is left free. Table 1 gives the relative voltage values present at various time instants.

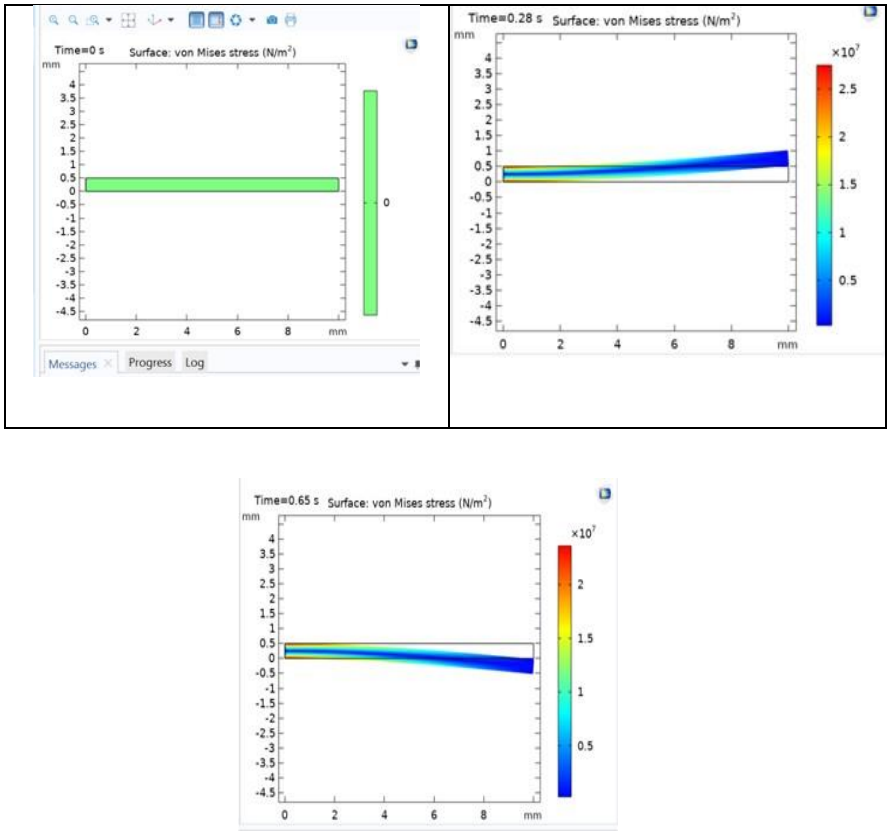

Fig. 3. Von Misses Stress (N/m2) Plot at different times on application of voltage

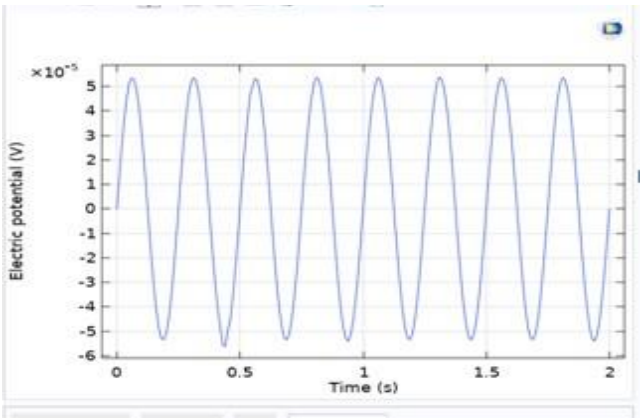

Fig. 4. Electric potential plot at different times

Table 1: Time vs voltage values

Index	Time (in sec)	Voltage (in V)
1	0	0.00000000000
2	0.01	0.00001333233
3	0.02	0.00002583610
4	0.03	0.00003671479
5	0.04	0.00004531194
6	0.05	0.00005160640
7	0.06	0.00005349044
8	0.07	0.00005273268
9	0.08	0.00004853435
10	1.95	-0.00005138532
11	1.96	-0.00004542439
12	1.97	-0.00003678336
13	1.98	-0.00002584108
14	1.99	-0.00001330991
15	2	-0.00000001539

IV.ii. Piezoacoustic simulation

The next part of the design model is a piezoelectric transducer to analyze the acoustic behavior of the piezoelectric material, here Aluminium Nitride, which is a new-age piezoelectric material that has very less harmful properties in comparison to PZT and other lead-based piezo materials. In this, a simple Aluminium Nitride structure of 1 mm length is chosen that has an acoustic shield air shown in Figure 4a below. The concentric circular part around this semicircular region is the Perfect Matched Layer that is used to record the disturbances of potential acoustic pressure as seen by the sensing element in an ultrasound-detecting device. The rectangular part shown in Figure 5a has 2-D Axial symmetry. When generating this geometry of the piezoelectric element let there is a consideration of acoustics over the entire cross-section except for the piezoelectric bar. Adding the height expression to the acoustic pressure domain of the Aluminium Nitride enclosure, Figure 4bdemonstrates the acoustic pressure wave at the end of the piezoelectric material that gives the required impact onto the perfectly matched layer. The results indicate the graphical analysis and give the numerical interpretation of how the elemental piezo electric transducer works in a real-time scenario of ultrasound acoustics at 200 kHz, ultrasound frequency as shown in Figure 4. The acoustic pressure shown above in Figure 4b, observed with a different colour, indicates the variation of the acoustic pressure that forms the basis for the image of ultrasound probes.

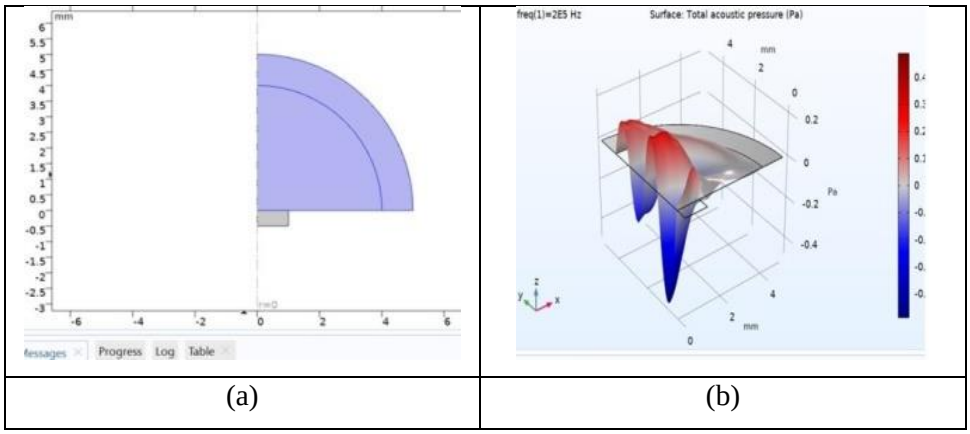

(a) (b)

Fig. 5. (a) Perfect Matched Acoustic Layer for a simple piezoelectric element (b) Acoustic Pressure used for Imaging

The comparison with the previously held materials, like PZT, is shown in the table below

Table 2: Comparison of AlN and PZT material for ultrasound probe

Parameter	Aluminum Nitride (AlN)	Lead Zirconate Titanate (PZT)
Piezoelectric Coefficient (d_{33})	~5 pm/V (lower)	~300-600 pm/V (higher)
Acoustic Impedance (Z)	~34 MRayl (closer to tissue)	~30-35 MRayl (but varies with composition)
Harmful Effects	Non-toxic, eco-friendly	Contains lead (toxic, environmental concerns)
Acoustic Pressure Wave Amplitude	Moderate (due to lower d_{33})	Higher (stronger piezoelectric response)
Signal Sensitivity	Good for high-frequency applications	Excellent due to high electromechanical coupling
Bandwidth	Wider (due to lower mechanical losses)	Narrower (higher damping)
Thermal Stability	High (stable at high temperatures)	Moderate (may depolarize at high temps)
Fabrication Compatibility	CMOS-compatible (good for MEMS)	Requires special handling (lead content)

V. Conclusion and Future Scope

The COMSOL simulation effectively demonstrated the interactions between electrical inputs and mechanical/acoustic outputs in piezoelectric materials. The analysis of piezo material provided valuable insights into the stress distribution and electric potential under operational conditions, while the acoustic an alysis of the Aluminium Nitride transducer highlighted its potential for ultrasound applications, especially given its environmentally friendly nature, low permittivity, and good thermalstability. This study underscores the importance of proper boundary conditions, meshing techniques, and material selection in accurately modelling and understanding the behavior of piezoelectric transducers. The established results in the work present an ultrasound frequency model of an elemental piezo-acoustic transducer-based probe. The simulation conducted at 200 kHz offers a foundational perspective on frequency performance in ultrasound devices, establishing a model approach that can be applied to other ultrasound range frequencies as well. The outcome of this approach is the amount of stress and acoustic pressure coming out of the piezomaterial noted after the 3D graphs. The 3D acoustic pressure simulations in the air medium give a perfectly matched layer to capture the piezo-acoustic vibrations. The acoustic pressure wave forms deduced from perfectly matched layers will give a plot of the imagery of an organ internal to the human body probed. The array of such a piezoelectric material structure can be formed to give high-resolution images from ultrasound imaging devices. With this study, we aim to provide valuable insights into the piezoacoustic behavior of Aluminum Nitride devices, which can inform the design and optimization of future radio frequency acoustic wave applications.

Conflict of Interest:

There was no relevant conflict of interest regarding this paper.

References

I. A. Abu-libdeh, and A. Emadi, “Piezoelectric Micro machined Ultrasonic Transducers (PMUTs): Performance Metrics, Advancements, and Applications,” *Sensors,* Vol: 22, no: 23, Nov. 2022. 10.3390/s22239151.

II. A. Guedes, et al., "Aluminum nitride pMUT based on a flexurally-suspended membrane,” *2011 16th International Solid-State Sensors, Actuators and Microsystems Conference*, Beijing, China, 2011, pp: 2062-2065. 10.1109/TRANSDUCERS.2011.5969223.

III. A. Iula, “Ultrasoundsystemsforbiometricrecognition,” *Sensors Review,* Vol: 19, no. 10, May 2019. 10.3390/s19102317

IV. A. Neprokin, C. Broadway, T. Myllylä, A. Bykov, and I. Meglinski, “Photoacoustic imaging in biomedicine and life sciences,” *Life,* Vol: 12, no: 4, p. 588, Apr. 2022. 10.3390/life12040588.

V. A. Safari, Q. Zhou, Y. Zeng, and J. D. Leber, "Advances in development of Pb-free piezoelectric materials for transducer applications," *Japanese Journal of Applied Physics*, Vol: 62, no: SJ, p: SJ0801, Mar. 2023. 10.35848/1347-4065/acc812.

VI. Akasheh,et al., "Development of Piezoelectric Micromachined Ultrasonic Transducers," *Sensors Actuators Applied Physics*. Vol: 111, pp: 275–287, Mar. 2024, 10.1016/j.sna.2003.11.022

VII. B. Herrera, P. Simeoni, G. Giribaldi, L. Colombo, and M. Rinaldi, "Scandium-Doped Aluminum Nitride PMUT Arrays for Wireless Ultrasonic Powering of Implantables," *IEEE Open Journal of Ultrasonics Ferroelectrics and Frequency Control*, Vol: 2, pp: 250–260, Jan. 2022. 10.1109/ojuffc.2022.3221708.

VIII. C. Cheng, "Piezoelectric Micromachined Ultrasound Transducers Using Lead Zirconate Titanate Films," Ph.D. dissertation, Dept. Materials Science and Engg., Pennsylvania State Univ., Pennsylvania, USA, 2021.

IX. C. Fei et al., "Ultrahigh frequency (100 MHz–300 MHz) ultrasonic transducers for optical resolution medical imagining," *Scientific Reports*, Vol: 6, no: 1, Jun. 2016. 10.1038/srep28360.

X. D. O. Urroz-Montoya, J. R. Alverto-Suazo, J. R. Garcfa-Cabrera, and C. H. Ortega-Jimenez, "Piezoelectricity: a literature review for power generation support,"MATEC Web of Conferences, Vol: 293, p: 05004, Jan. 2019. 10.1051/matecconf/201929305004.

XI. E. G. Nesvijski, "Some aspects of ultrasonic testing of composites," *Composite Structures*, Vol: 48, pp:151–155, Mar 2000, 10.1016/S0263-8223(99)00088-4

XII. E. Ledesma, I. Zamora, A. Uranga, F. Torres, and N. Barniol, "Enhancing AlN PMUTs' Acoustic Responsivity within a MEMS-on-CMOS Process," *Sensors*, Vol: 21, no. 24, p. 8447, Dec. 2021. 10.3390/s21248447.

XIII. F. Pop, B. Herrera, and M. Rinaldi, "Lithium Niobate Piezoelectric Micromachined Ultrasonic Transducers for high data-rate intrabody communication," *Nature Communications*, Vol: 13, no: 1, Apr. 2022. 10.1038/s41467-022-29355-9.

XIV. F. Pop, B. Herrera, C. Cassella, and M. Rinaldi, "Modeling and optimization of directly modulated piezoelectric micromachined ultrasonic transducers," *Sensors*, Vol: 21, no: 1, p: 157, Dec. 2020. 10.3390/s21010157.

XV. H. Wang, "Development of Piezoelectric Micromachined Ultrasonic Transducers (Pmuts) For Endoscopic Photoacoustic Imaging Applications," Ph.D. dissertation, Dept. Electri. and Comp. Engg., University Of Florida, Gainesville, Florid, USA, 2021.

XVI. H. Wang, Z. Chen, H. Yang, H. Jiang, and H. Xie, "A ceramic PZT-Based PMUT array for endoscopic photoacoustic imaging," *Journal of Microelectromechanical Systems*, Vol: 29, no. 5, pp: 1038–1043, Jul. 2020. 10.1109/jmems.2020.3010773.

XVII. J. Cai et al., "Photoacoustic imaging based on broadened bandwidth aluminum nitride piezoelectric micromachined ultrasound transducers," *IEEE Sensors Letters*, Vol: 7, no: 4, pp: 1–4, Mar. 2023. 10.1109/lsens.2023.3254593

XVIII. J. Jung, W. Lee, W. Kang, E. Shin, J. Ryu, and H. Choi, "Review of piezoelectric micromachined ultrasonic transducers and their applications," *Journal of Micromechanics and Microengineering*, Vol: 27, no: 11, p; 113001, Aug. 2017. 10.1088/1361-6439/aa851b

XIX. J. Kim et al., "A Rapid Prototyping Method for Sub-MHz Single-Element Piezoelectric Transducers by Using 3D- Printed Components," *Sensors*, Vol: 23, no: 1, Dec 2022. 10.3390/s23010313

XX. J. Pan, C. Bai, Q. Zheng, and H. Xie, "Review of Piezoelectric Micromachined Ultrasonic Transducers for Rangefinders," *Micromachines*, Vol: 14, no: 2, p: 374, Feb. 2023. 10.3390/mi14020374.

XXI. J. Y. Pyun, Y. H. Kim and K. K. Park. "Design of Piezoelectric Acoustic Transducers for Underwater Applications," *Sensors*, Vol: 23, no. 4, Feb. 2023. 10.3390/s23041821

XXII. J.E.Aldrich, "Basic Physics of Ultrasound Imaging," *Crit. Care Med*., Vol: 35 pp: S131–S137, May 2007. 10.1097/01.ccm.0000260624.99430.22.

XXIII. M. Darmon, G. Toullelan and V.Dorval, "An Experimental and Theoretical Comparison of 3D Models for Ultrasonic Non-Destructive Testing of Cracks: PartI, Embedded Cracks," *Applied Sciences*, Vol:12, no: 10, May 2022. 10.3390/app12105078

XXIV. M. Ishikawa et al., "Lead Zirconate Titanate Thick-Film Ultrasonic Transducer for 1to20MHz Frequency Bands Fabricated by Hydrothermal Polycrystal Growth," *Japanese Journal of Applied Physics*, Vol: 44, no: 6S, pp:4342, Jun. 2005. 10.1143/JJAP.44.4342

XXV. M.Lethiecq et al., Piezoelectric Transducer Design for Medical Diagnosis and NDE", *Piezoelectric and Acoustic Materials for Transducer Applications, Springer* US, pp:191-215,2008. 10.1007/978-0-387-76540-2_10

XXVI. Q. Yu *et al.*, "PZT-Film-Based Piezoelectric Micromachined Ultrasonic Transducer with I-Shaped Composite Diaphragm," *Micromachines*, Vol: 13, no: 10, p: 1597, Sep. 2022. 10.3390/mi13101597.

XXVII. Q.Zhouetal.,"Piezoelectric Single Crystal Ultrasonic Transducers for Biomedical Applications," *Prog. Mater. Sci.* Vol:66, pp: 87–111, Oct. 2014. 10.1016/j.pmatsci.2014.06.001

XXVIII. R. Manwar, K. Kratkiewicz, and K. Avanaki, "Overview of Ultrasound Detection Technologies for Photoacoustic Imaging," *Micromachines*, Vol: 11, no: 7, p: 692, Jul. 2020. 10.3390/mi11070692.

XXIX. W. Lee,and Y .Roh, "Ultrasonic transducers for medical diagnostic imaging," *Biomedical Engineering Letters*, Vol: 7, pp: 91–97, Mar. 2017.10.1007/s13534-017-0021-8

XXX. Xin Su et al., "Simulation and Optimization of Piezoelectric Micromachined Ultrasonic Transducer Unit Based on AlN," *Electronics*, Vol:11, no: 18. 2022. 10.3390/electronics11182915

XXXI. Y. Li, T. Omori, K. Watabe and H. Toshiyoshi, "Bandwidth and Sensitivity Enhancement of Piezoelectric MEMS Acoustic Emission Sensor Using Multi-Cantilevers,"*2022 IEEE 35th International Conference on Micro Electro Mechanical Systems Conference (MEMS)*, Tokyo, Japan, 2022, pp: 868-871. 10.1109/MEMS51670.2022.9699581.

XXXII. P. Muralt et al., "Recent Progress in Materials Issues for Piezoelectric MEMS", *Journal of the American Ceramic Society*, 91 (5) pp: 1385-1396, 2008. 10.1111/j.1551-2916.2008.02421.x

XXXIII. G. Piazza et al., "A Study on the Effects of Bottom Electrode Designs on Aluminum Nitride Contour-Mode Resonators", *Journal of Micromachines*, Volume 10, Issue 11, Article 758, 2019. 10.3390/mi10110758

XXXIV. Sherrit et al., "Characterization of Piezoelectric Materials for Transducers", *Dielectric and Ferroelectric Reviews* (via arXiv 0711.2657), 2012. 10.48550/arXiv.0711.2657

XXXV. Tadigadapa, S. et al., "Piezoelectric MEMS sensors: State-of-the-art and perspectives", *Measurement Science and Technolog*, Volume 20 (Issue 9), Article ID 092001, 2009. 10.1088/0957-0233/20/9/092001

XXXVI. K. Kirk Shung et al., "Diagnostic Ultrasound: Imaging and Blood Flow Measurements", *CRC Press (Taylor & Francis Group)*, ***Boca Raton***, April 1, 2015. 10.1201/9780849338922

XXXVII. W.A.Smith et al., "Modeling 1-3 Composite Piezoelectrics: Thickness-Mode Oscillations", *IEEE Transactions on Ultrasonics, Ferroelectrics, and Frequency Control*, Volume 38, **Issue:** 1, **Pages:** 40–47, January 1991. 10.1109/58.67833